Reactivity landscape of pyruvate under simulated hydrothermal vent conditions

Yehor Novikov[a] and Shelley D. Copley[b,c,1]

[a]Department of Chemistry and Biochemistry, [b]Department of Molecular, Cellular, and Developmental Biology, and [c]Cooperative Institute for Research in Environmental Sciences, University of Colorado Boulder, Boulder, CO 80309

Pyruvate is an important "hub" metabolite that is a precursor for amino acids, sugars, cofactors, and lipids in extant metabolic networks. Pyruvate has been produced under simulated hydrothermal vent conditions from alkyl thiols and carbon monoxide in the presence of transition metal sulfides at 250 °C [Cody GD et al. (2000) *Science* 289(5483):1337–1340], so it is plausible that pyruvate was formed in hydrothermal systems on the early earth. We report here that pyruvate reacts readily in the presence of transition metal sulfide minerals under simulated hydrothermal vent fluids at more moderate temperatures (25–110 °C) that are more conducive to survival of biogenic molecules. We found that pyruvate partitions among five reaction pathways at rates that depend upon the nature of the mineral present; the concentrations of H_2S, H_2, and NH_4Cl; and the temperature. In most cases, high yields of one or two primary products are found due to preferential acceleration of certain pathways. Reactions observed include reduction of ketones to alcohols and aldol condensation, both reactions that are common in extant metabolic networks. We also observed reductive amination to form alanine and reduction to form propionic acid. Amino acids and fatty acids formed by analogous processes may have been important components of a protometabolic network that allowed the emergence of life.

catalysis | prebiotic chemistry | abiogenesis

Baross and Hoffman suggested in 1985 that life emerged in or around hydrothermal vents from a protometabolic network fueled by small molecules such as CO_2, NH_3, and H_2 in hydrothermal fluids (1). The existence of dense biological communities sustained solely by the chemicals and energy provided by vent fluids proves that these habitats are capable of supporting life. The possibility that life originated at such sites is appealing for a number of reasons. Pores in vent walls and the surrounding fractured crust could have provided compartmentalization before the availability of lipid membranes. The mineral surfaces lining these compartments could have catalyzed the formation of organic compounds from the constituents of vent fluids. Temperature gradients in hydrothermal systems could have allowed reactions with high activation energies to occur in the internal hot regions as well as formation of more fragile molecules near the cool outer wall. In addition, both theoretical and experimental studies have demonstrated that thermal gradients can lead to massive concentration of molecules in small regions of microchannels due to a combination of convection and thermophoresis (2, 3). This physical mechanism would enhance the rates of second-order reactions between molecules originating from chemical reactions in hydrothermal fluids as they percolate through pores and channels in vent structures and in cracks in the surrounding crust.

An important challenge for prebiotic chemists is to explore the potential for synthesis of complex organic molecules from geochemical precursors in hydrothermal environments. In this work, we have begun to explore the differential abilities of minerals to catalyze reactions that could have been involved in a protometabolic network that set the stage for the emergence of life. Although the importance of rate acceleration by catalysts is obvious, a less-appreciated role for early catalysts would have been to prune complex protometabolic networks, allowing accumulation of higher concentrations of a few components, rather than low

concentrations of many components (4). Fig. 1 shows an example in which the availability of catalysts for different steps in a network results in significantly different network topologies and accumulation of different products. Network topology also depends on the set of reagents available and the concentrations of those reagents. For example, the network depicted in Fig. 1 would form only **K** and **M** if no **H** were available, and would form only **J** and **M** if the concentration of **H** were very high (assuming equal rate constants for the partitioning of **D** between the two possible pathways).

The potential role of mineral surfaces during the emergence of life has been the subject of extensive writings by Wächtershäuser (5), Russell and coworkers (6), and Cody and coworkers (7, 8), among others. Mineral surfaces can catalyze reactions by concentrating reactants on surfaces, polarizing functional groups to enhance partial charges and thereby facilitating attack by other species, stabilizing reaction intermediates, and transferring electrons. The catalytic power of metal ions and clusters has been exploited by numerous metalloenzymes (9) as well as industrial processes (10).

A wide range of minerals exists at current hydrothermal vents. Transition metal sulfides such as pyrrhotite (FeS), pyrite (FeS_2), chalcopyrite ($CuFeS_2$), sphalerite ((Zn,Fe)S), and often smaller quantities of arsenopyrite (FeAsS) are found in vents at mid-ocean spreading centers (e.g., the Juan de Fuca Ridge) (11). At these sites, hot fluids (up to 400 °C) laden with transition metals, CO_2, H_2S, and H_2, vent into cool ocean water, leading to precipitation of towers composed primarily of transition metal sulfides. Clay minerals such as nontronite (12) and phyllosilicates such as chlorite (13) are also found in these hydrothermal systems. Secondary minerals such as zeolites that are produced upon reaction of hot basalt melts with seawater are frequently observed together with sulfide minerals. For instance, clinoptilolite occurs at the Juan de Fuca Ridge (14) and stilbite was detected on the ocean floor at 1.1 km depth along with pyrite (15).

A fundamentally different type of vent is found in peridotite-hosted systems (e.g., the Lost City) (16, 17) found off the main spreading axis. At these sites, reactions between seawater and newly exposed mantle olivine [$(Mg,Fe)_2SiO_4$] generate serpentine [$Mg_3Si_2O_5(OH)_4$], magnetite (Fe_3O_4), and alkaline fluids that, upon mixing with cool seawater, generate towers from precipitation of aragonite ($CaCO_3$) and brucite [$Mg(OH)_2$]. Serpentine undergoes further reaction with CO_2 to give talc [$(Mg_3Si_4O_{10}(OH)_2$]. Vent fluids are cooler in these systems (< 90 °C), and are rich in H_2 and CH_4.

We have begun to explore the catalytic landscape provided by hydrothermal vents by characterizing the products formed from pyruvate in the presence of transition metal sulfide minerals. Pyruvate is of particular interest in prebiotic chemistry because in extant metabolic networks it undergoes various reactions
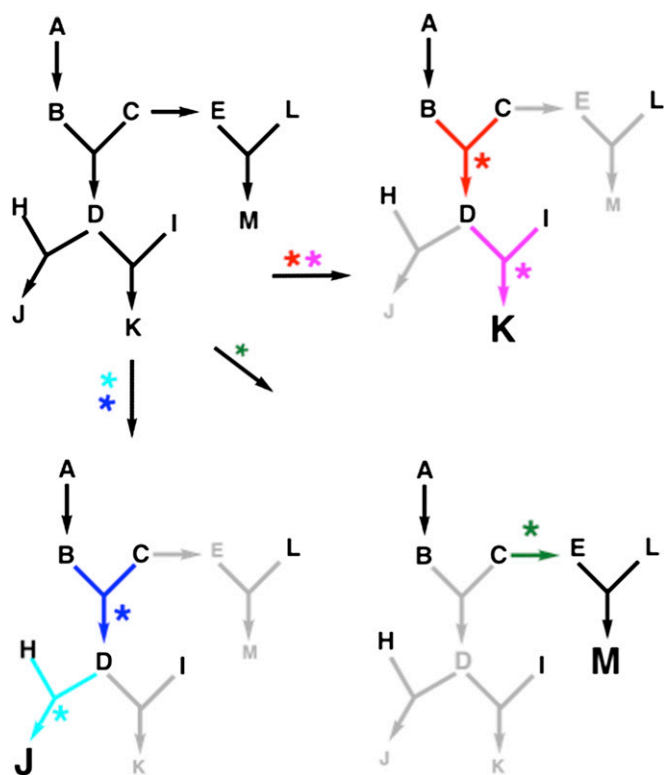
Fig. 1. The presence of different catalysts (colored asterisks) that accelerate particular reactions (colored arrows) prunes a complex reaction network to a simpler network in which higher concentrations of particular products can be formed.

leading to amino acids, sugars, cofactors, and lipids. Further, Cody et al. have shown that small amounts of pyruvate can be produced under simulated hydrothermal vent conditions from alkyl thiols and carbon monoxide in the presence of transition metal sulfides at 250 °C (18). We are interested in products that might be formed from pyruvate in cooler regions of vent walls in which more fragile molecules might be stable. Because vent walls are porous, some of the hot hydrothermal fluid percolates through regions of the wall that are cooler due to contact with cold seawater. Consequently, molecules that form in the high-temperature regions of the wall may undergo additional reactions as they move toward the cooler exterior wall.

The composition of vent fluids in extant hydrothermal systems varies considerably (11). We have begun our studies with a simplified system containing transition metal sulfides and pyruvate in the presence of CO_2, H_2, H_2S, and, in some cases, NH_4Cl, at pH 4. We used a concentration of CO_2 (100 mM) within the range of those found in hydrothermal fluids from black smokers (4–215 mM) (6). We were particularly interested in whether any of the minerals might catalyze carboxylation of pyruvate to oxaloacetate, a precursor of aspartate, and an intermediate in the tricarboxylic acid cycle. However, we detected no products formed by carboxylation reactions, so CO_2 apparently did not participate as a reactant in our system. The concentration of H_2 in fluids from black smokers ranges from 0.1 to 50 mM (6); we used 100 mM in our experiments. The concentration of H_2S (20 mM) we used was within the range observed in fluids from black smokers (3–110 mM) (6). NH_4Cl (70 mM) was included in some reactions to examine the potential for reductive amination of pyruvate to alanine. A relevant concentration of NH_3 is difficult to predict. However, reduction of N_2 to NH_3 by minerals under high-temperature and high-pressure conditions has been demonstrated and proposed to provide the major source of reduced nitrogen on the early earth (19). Reduced nitrogen was certainly available on the early earth, although

concentrations likely varied widely between hydrothermal sites. The experimental conditions we used do not mimic those found at any particular extant vents, which are complex structures with mixtures of minerals that change over time, as does the composition of the vent fluids (11). The composition of vents and vent fluids may have been different on the primordial earth when the ocean was anoxic and slightly acidic. However, this initial exploration suffices to demonstrate the types of products that are accessible in the presence of transition metal sulfide minerals and to demonstrate the dependence of reaction network topology upon the type of mineral present, the concentrations of each reactant in the system, and the temperature and pH.
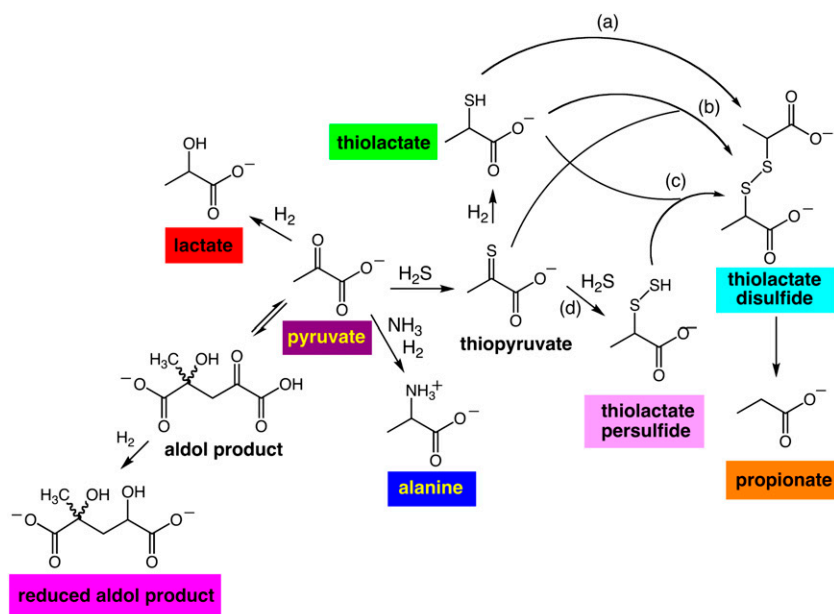
Products formed from pyruvate in the presence of powdered minerals after reaction for 24 h at either 25 or 110 °C in a Teflon tube enclosed in a pressurized reactor were recovered and analyzed by NMR spectrometry and mass spectroscopy. Under the various conditions we explored, we identified nine products that were formed in yields ranging from 0.1 to 60% based upon the initial pyruvate concentration (Fig. 2). These results demonstrate that pyruvate can undergo a range of chemical reactions in the presence of mineral catalysts at moderate temperatures. Further, the suite of products formed depended upon the nature of the catalyst, the temperature, and the presence or absence of ammonia.

Results and Discussion

Reactor for Studying Reactions under High Pressure. We designed and constructed a reactor for carrying out reactions under high pressure (Fig. 3, enlarged version in Fig. S1). The vessel contains a 1-mL Teflon sample tube (OD 5/16 inch, ID 1/4 inch, height 2 inches) to prevent contact of reaction mixtures with the walls of the vessel, a valve for introducing gases, and a mechanism for achieving the desired pressure. This reactor is an improvement over previous approaches that have relied upon in situ generation of gases such as CO (from formic acid) (7) and H_2S (from Na_2S and NH_4Cl or acetic acid) (20) because it allows direct introduction of gases at desired compositions and pressures. Furthermore, the use of sealed Teflon reaction tubes within the pressure vessel prevents contact of the solution with metal surfaces that might catalyze adventitious reactions. The reactor can be easily and safely pressurized to 1,000 atm and heated up to 180 °C. The deepest known black smoker system is found at 5000 m in the Cayman Trough in the Caribbean, a depth at which the pressure is ~500 atm (21). Thus, the reactor can achieve pressures commensurate with those found in extant vent systems. Most importantly, this allows introduction of gases into the system at levels as high (or higher) than those found in extant vents.

To carry out reactions under simulated hydrothermal vent conditions, a 1-mL slurry of powdered mineral (100 mg) and reactants was loaded into the sample tube in an anoxic glovebox along with a small smooth alumina ball to allow mixing. The vessel was closed and removed from the glovebox. The required gases were introduced into the headspace above the reaction mixture through a valve below the moveable Teflon plug. The chamber was pressurized by screwing a piston downward until the desired pressure was reached. This action also forces the Teflon plug into the sample tube to seal the reaction chamber. The vessel was rocked back and forth to allow mixing for 24 h at the desired temperature.

Reaction products were analyzed by a painstaking process developed to ensure high recovery of reaction components, with particular attention to maintenance of anoxic conditions while reaction mixtures were in contact with mineral catalysts. After 24 h, reaction mixtures were recovered from the reactor and diluted to ~5 mL with distilled water. At this point, the pH of the solution was 3.5–5.0. A few boiling chips were added and the slurry was immediately introduced into a glovebox antechamber. Dissolved gases were removed by three cycles of evacuation and purging with argon. The slurry was then transferred into the glove box and the pH adjusted to 9.5–10 to remove soluble metal ions leached from the minerals by precipitation as metal hydroxides. Subsequently, the slurry was filtered and the pH was adjusted to 7.5 ± 0.1. The solution was removed from the glovebox.

Fig. 2. Structures of products formed from pyruvate. Aldol condensation product, 2-hydroxy-2-methyl-4-oxo-pentanedioate; reduced aldol product, 2-hydroxy-2-methyl-4-hydroxypentanedioate. *A* indicates a reaction that proceeds via recombination of two sulfur radicals; *B* and *D* indicate reactions that occur via thiophilic attack on thiopyruvate; *C* indicates a reaction that results from nucleophilic attack of thiolactate on the proximal sulfur of thiolactate persulfide. For purposes of simplification, reaction byproducts are not shown.

Reaction products were characterized by ^{1}H- and ^{13}C-NMR spectroscopy and mass spectrometry. Two-dimensional NMR techniques were used for assignment of peaks in complex mixtures. An example is shown in Fig. S2.

To ensure that products observed were produced from pyruvate rather than reaction of organic material associated with the minerals, we carried out a number of reactions using fully labeled ^{13}C-pyruvate. An example is shown in Fig. S3. The splitting of each proton signal due to the adjacent ^{13}C indicates that all of the products observed were fully labeled with ^{13}C. Subsequent reactions were carried out with unlabeled pyruvate.

Control Reactions in the Absence of Minerals. When pyruvate was incubated in the reactor in the presence of 100 mM H_2, 100 mM CO_2, and 20 mM H_2S, but no mineral, the majority of the pyruvate was recovered intact. Small amounts of products of thiolactate disulfide and thiolactate persulfide were detected (Fig. 4*A* and Table S1). Additional experiments demonstrated that H_2 was not required for formation of these products, indicating that the necessary reducing equivalents, at least for some potential reaction pathways, can be derived from H_2S.

Analysis of Recovery and Reproducibility in the Presence of Minerals. The reproducibility of our analytical procedures was examined by carrying out reactions in the presence of pyrite four times. As shown in Table 1, both the overall recoveries and the yields of individual products showed good reproducibility, especially considering the heterogeneous reaction mixture and required workup. Even components formed in small amounts (0.1–0.2%, corresponding to 0.4–0.8 mM) were detected reproducibly. Similar reproducibility was seen in four replicates of a comparable experiment with pyrrhotite (Table S1). In both cases, the missing material may have been tightly bound to the mineral surface, or may have been volatile and removed during the evaporation steps of the workup. However, the several products that are consistently detected allow important conclusions to be made about the reactivity landscape of pyruvate under simulated hydrothermal conditions.

Reduction of Pyruvate to Lactate. Pyruvate was converted to lactate in high yield by pyrrhotite ($Fe_{1-x}S$, where $x = 0–0.2$) obtained from Aldrich in the presence of 100 mM H_2, 100 mM CO_2, and 20 mM H_2S for 24 h even at room temperature (Fig. 4*A* and Table S1). Because the commercial pyrrhotite contained a number of trace contaminants, we also investigated this reaction

using highly purified synthetic FeS (troilite). In the presence of troilite, 133 mM H_2, 100 mM CO_2, and 5 mM H_2S (concentrations chosen to favor the reduction of pyruvate over the competing conversion to thiolated products), efficient reduction of pyruvate to lactate was still observed, suggesting that the reduction observed with pyrrhotite was not due to trace metal contaminants in the mineral or to defects in the crystal lattice due to insufficient Fe. Lower yields of lactate were obtained in the presence of arsenopyrite (FeAsS). Note that the yields of products are not an indication of the intrinsic reactivities of the various minerals, as the surface areas of the different minerals used in the reactions were not the same. Rather, it is the partitioning of products along various pathways that is relevant.

Only trace amounts of lactate were formed in the presence of pyrite and 100 mM H_2, 100 mM CO_2, and 20 mM H_2S at either 25 or 110 °C (Fig. 4*A*). However, lactate was formed in 18% yield in comparable reactions carried out in the presence of 70 mM NH_4Cl at 110 °C (Fig. 4*B*). This result suggests that NH_4Cl may catalyze the reduction of lactate, possibly by serving as a proton
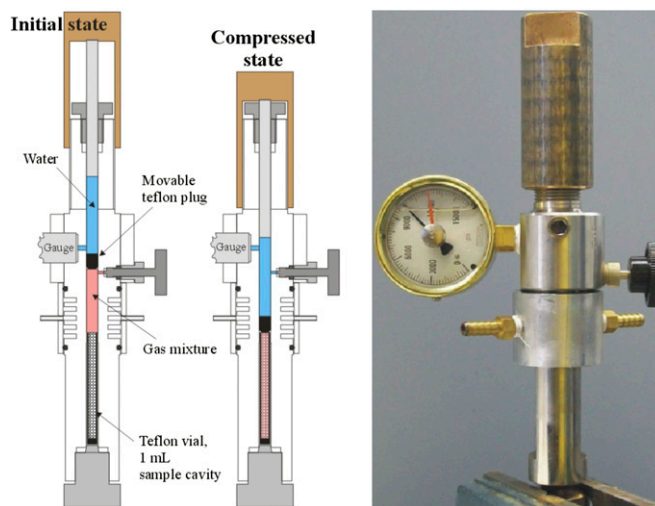
Fig. 3. Schematic and photograph of a custom-built reactor for carrying out reactions under high pressure with defined mixtures of gases introduced through valves as indicated.
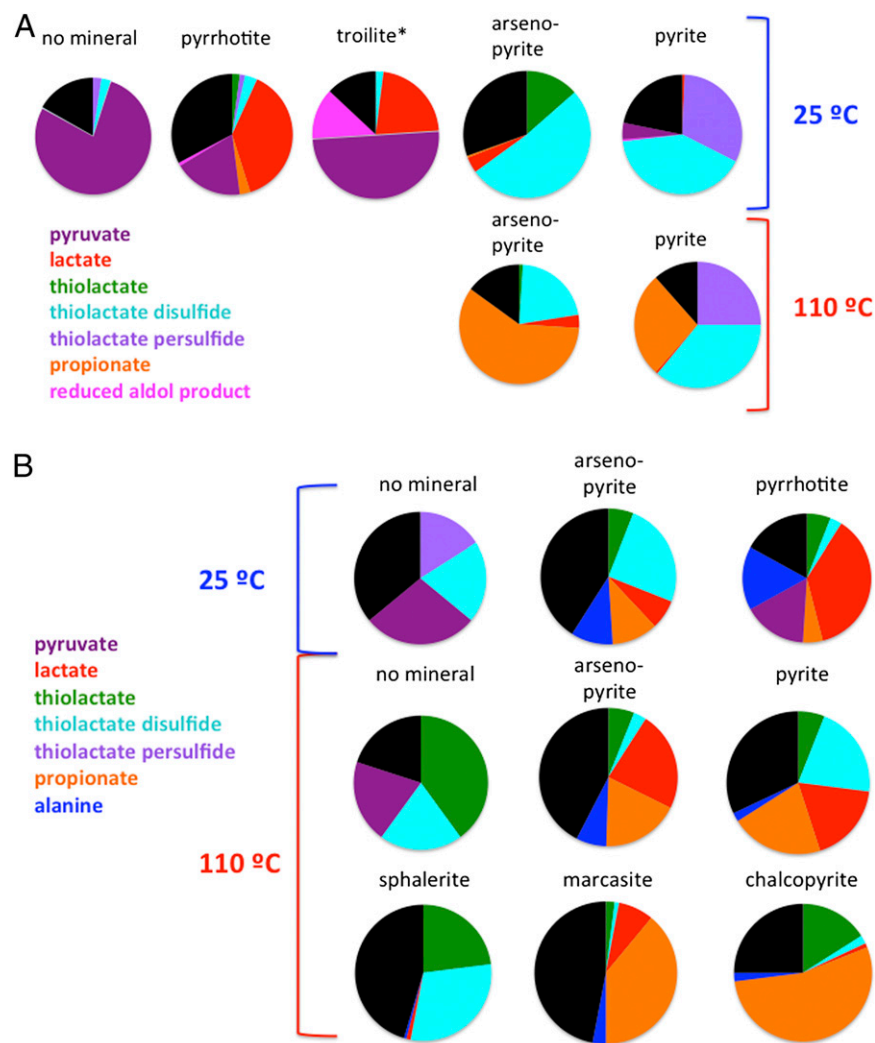
Fig. 4. (*A*) Summary of the yields of products detected after incubation of pyruvate with various minerals at 25 °C (*Upper*) and at 110 °C (*Lower*) in the presence of 100 mM H_2, 20 mM H_2S, and 100 mM CO_2. Black indicates missing material based upon the initial concentration of pyruvate. Other colors correspond to those used in Fig. 2. *The reaction with troilite was carried out using 133 mM H_2, 5 mM H_2S, and 100 mM CO_2. (*B*) Summary of the yields of products detected after incubation of pyruvate with various minerals at 25 °C (*Top*) and at 110 °C (*Middle* and *Bottom*) in the presence of 70 mM NH_4Cl, 100 mM H_2, 20 mM H_2S, and 100 mM CO_2. Black indicates missing material based upon the initial concentration of pyruvate. Other colors correspond to those used in Fig. 2.

donor. More generally, this result underscores the potential synergism between small molecule and transition metal sulfide catalysts.

It is interesting that less lactate is formed in the presence of marcasite than in the presence of pyrite when NH_4Cl is present. In fact, the overall distribution of products is quite different in the two cases. Marcasite and pyrite are both FeS_2, but marcasite has an orthorhombic lattice whereas pyrite has a cubic lattice. This finding demonstrates the important role that the crystal lattice plays; this is likely due in part to differences in proximity and orientation of substrates that are associated with the surface and the molecules that participate in the reaction, including transition metal ions that may polarize the carbonyl and facilitate nucleophilic attack. It is interesting to note that the [4Fe-4S] clusters found in extant metalloenzymes, including nitrogenase (the enzyme responsible for fixing N_2) and CO dehydrogenase (which is

involved in one of several extant pathways for carbon fixation) and hydrogenases (which catalyze the reversible reduction of protons to H_2), are present in cubane-like structures (9, 22).

To probe the mechanism of the reduction of pyruvate to lactate, the reaction was carried out in the presence of FeS, H_2, and D_2O. Mass-spectroscopic analysis demonstrated that 90% of the lactate formed had incorporated deuterium rather than hydrogen at carbon-2. Analysis of the recovered gas mixture revealed only minimal (< 3%) exchange of deuterium into H_2. These results preclude mechanisms involving direct addition of H_2 or D_2 across the double bond of pyruvate. Rather, reduction of pyruvate must occur either by electron transfer followed by protonation by the solvent or by initial formation of a hydride species on the surface that exchanges rapidly with the solvent before transfer to the carbonyl carbon of pyruvate.

Table 1. Recovery of pyruvate and reaction products from replicate reactions carried out with 100 mg/mL pyrite, 100 mM H_2, 100 mM CO_2, and 20 mM H_2S at 25 °C for 24 h

Pyruvate	Lactate	Thiolactate persulfide	Thiolactate disulfide	Aldol product	Propionate	Total recovery
6	0.6	25	33	0.5	0.0	64
3	0.4	29	49	0.8	0.0	85
2	0.7	38	36	0.5	0.2	77
7	1.0	35	44	0.0	0.2	86
4.5 ± 1.2	0.68 ± 0.13	32 ± 3	41 ± 4	0.5 ± 0.17	0.1 ± 0.06	78 ± 5

Product yields are expressed in terms of the percent of pyruvate converted to that product.

Reduction of carbonyl compounds to alcohols is a common reaction in extant metabolic networks, although the reducing equivalents are transferred as a hydride from reduced nicotinamide cofactors (NADH and NADPH). We are not aware of any previous demonstration of the reduction of pyruvate to lactate by minerals under simulated hydrothermal vent conditions. Although hydrogenation of C-O double bonds is a standard reaction in synthetic organic chemistry, the primary effort in that field has been to develop soluble and asymmetric catalysts (23).

Aldol Condensation of Pyruvate. We observed a small amount of the aldol-condensation product 2-hydroxy-2-methyl-4-oxopentanedioate during reactions of pyruvate in the presence of pyrrhotite (FeS obtained from Aldrich), 100 mM H_2, 100 mM CO_2, and 20 mM H_2S at 25 °C (Fig. 4A and Table S1). To probe this reaction further, we carried out a slightly modified reaction using synthetic FeS (troilite), 100 mM CO_2, 133 mM H_2, and 5 mM H_2S. (The concentration of H_2S was lowered in this experiment to decrease the rate of formation of thiolated products.) Under these conditions, we observed a substantial amount of the reduced aldol product (13% yield). This is a remarkable result, as aldol condensation reactions do not typically occur under mildly acidic conditions. Aldol condensation requires initial deprotonation of a molecule of pyruvate to form an enolate that can attack a second molecule of pyruvate. Both of these steps could conceivably be accelerated by the mineral surface. The observation of a substantial amount of the reduced aldol product suggests that the irreversible reduction of the aldol-condensation product pulled the condensation reaction toward a stable product. Aldol condensation is an important mechanism for formation of carbon–carbon bonds in extant metabolism, and the possibility that it could have occurred under mildly acidic conditions when H_2S concentrations were relatively low expands the range of geochemical conditions under which this reaction might have occurred. A further intriguing possibility is that formation of the enolate of pyruvate in the presence of a primordial phosphate donor (possibly polyphosphate) might have generated phosphoenolpyruvate, a precursor of sugars and aromatic amino acids in extant metabolism.

Formation of Thiolated Products. Strikingly different products from those described in the previous section were observed when reactions were carried out in the presence of pyrite at 25 °C. Only small amounts of lactate were formed. Rather, the presence of pyrite increased the formation of thiolactate persulfide and thiolactate disulfide. Substantial amounts of thiolactate persulfide were not found in the presence of other minerals (Fig. 4A and Table S1). This phenomenon could be due to preferential conversion of pyruvate to other products, or to efficient catalysis of the conversion of thiolactate persulfide to other products. It is intriguing to note that the presence of NH_4Cl increased the amounts of thiolactate persulfide and thiolactate disulfide formed in the control reaction in the absence of mineral (Fig. 4B and Table S2), suggesting that NH_4Cl might also catalyze one or more pathways leading to these products. Further, the formation of thiolated products in the absence of mineral demonstrates that H_2S can provide the sulfur in these products.

Thiolactate disulfide was found in reactions carried out with several minerals. As shown in Fig. 2, this product could be formed via multiple pathways through an unstable thiopyruvate intermediate. Small quantities of thiopyruvate were detected directly by mass spectrometry (exact mass 102.986). The signal from this peak shifted by 3 amu when U-^{13}C-pyruvate was used. However, thiopyruvate could not be detected by NMR. This is not surprising given the instability of thioketones, which is due to poor overlap between the carbon 2p orbital and the sulfur 3p orbital that form the π bond (24). The plausibility of the proposed intermediacy of thiopyruvate is supported by the similarities between our reaction conditions and those sometimes used to synthesize thioketones from ketones (reaction with H_2S in the presence of an acid catalyst, ref. 24). Notably, nucleophilic attack on thioketones can occur at the sulfur (25), so attack by a sulfide

on the sulfur of thiopyruvate could contribute to the formation of thiolactate disulfide and thiolactate persulfide.

The involvement of thiyl radicals (pathway a) is supported by the observation that addition of hydroquinone or 20 mM 4-hydroxy-2,2,6,6-tetramethylpiperidin-1-oxyl (4-hydroxy-TEMPO), a stable free radical that promotes free radical reactions, to a control reaction in the absence of mineral more than doubled the yield of thiolactate disulfide (Table S3). Simple nucleophilic attack of thiolactate on thiolactate persulfide (pathway c) is an obvious pathway for formation of thiolactate disulfide. Finally, thiophilic attack of a sulfide on thiopyruvate (pathways b and d) is a plausible route for formation of both thiolactate persulfide and thiolactate disulfide. It is notable that such reactions are unknown in extant biochemistry, probably because of the instability of thioketones, yet they form disulfides, which play important roles in extant metabolism and regulation.

Reactions carried out in the presence of arsenopyrite (FeAsS) at 25 °C resulted in yet another distinctive mixture of products. Thiolated products predominated, but in contrast to the case with pyrite, the major products were thiolactate disulfide and thiolactate. Thiolactate is apparently converted to thiolactate disulfide with high efficiency. It is notable that a small amount of lactate was also formed, suggesting that arsenopyrite is capable of catalyzing the hydrogenation reaction, but that the reaction leading to thiolactate is faster under these reaction conditions.

Formation of disulfide and persulfide products from ketones has been previously reported. Kaschke et al. (20) examined the products formed from cyclohexanone in the presence of $FeCl_2$ and H_2S in dimethylformamide after reaction at 25 °C. The major product formed under these conditions was dicyclohexane disulfide. Cyclohexyl persulfide was also formed.

The facile formation of thiolated products under all of the conditions we tested is interesting because of the pervasive presence of thiols in extant biochemistry. The thiol-containing amino acid cysteine is commonly used as a nucleophile in enzymatic reactions. Conversions between thiols and disulfides are involved in numerous metabolic reactions as well as protection against oxidative stress. Thioesters (acetyl CoA and malonyl CoA) are the precursors for fatty acid synthesis in bacteria and eukaryotes. Acetyl CoA is the primary acetylating "reagent" used in all domains of life (26–28). Finally, the thioether S-adenosylmethionine (SAM) is a universal methyl group donor, as well as a cofactor in the radical SAM superfamily of enzymes (29, 30). The plethora of roles for thiols in extant metabolism suggests that life originated in a sulfur-rich environment in which incorporation of sulfide into organic molecules was readily accomplished.

Pyruvate Is Converted to Propionate at Higher Temperatures. Formation of a small amount of propionate was observed after reactions of pyruvate in the presence of pyrrhotite, pyrite, and arsenopyrite at 25 °C (Fig. 4A and Table S1). The formation of propionate showed a dramatic dependence on temperature; when the temperature was increased to 110 °C, propionate was formed with a yield of 27% in the presence of pyrite and 63% in the presence of arsenopyrite (Fig. 4A and Table S1). Substantial amounts of propionate were also formed in the presence of marcasite and chalcopyrite, but not sphalerite (Fig. 4B and Table S2). (The latter reactions were carried out in the presence of 70 mM NH_4Cl.) Precedent for this reaction is found in a study that investigated the products formed from phenylpyruvate after incubation with FeS and H_2S at 100 °C (31), conditions that result in formation of pyrite and H_2 and are thus similar to those we used for the reaction in the presence of pyrite. After 12 d, a 24% yield of phenylpropionate was detected. Reduction of pyruvate to propionate appears to be a dominant reaction at high temperatures in the presence of transition metal sulfides that contain iron, including chalcopyrite, which contains both copper and iron. The presence of H_2S is important for this reaction because it results in formation of thiolactate disulfide, a direct precursor of propionate (Fig. 2), based upon the observation that incubation of thiolactate disulfide with pyrrhotite, 100 mM CO_2 and 133 mM H_2

for 24 h at 100 °C gave a 15% yield of propionate with no other products (Table S4). In contrast, lactate, which would be a major product in the absence of H_2S, can be eliminated as a precursor of propionate because no propionate was formed during incubation of lactate with FeS, 100 mM CO_2, and 133 mM H_2 at 100 °C. This finding is particularly significant because it provides a mechanism for conversion of α-keto acids to fatty acids; formation of longer chain fatty acids by this process could have provided a primordial source of material for the first bilayer membranes.

Reductive Amination of Pyruvate to Alanine. Incorporation of nitrogen into organic molecules was critical for the emergence of life, as the amino acid and nucleobase precursors of macromolecules contain nitrogen that is incorporated in extant organisms from ammonia. Consequently, we explored the effect of addition of NH_4Cl (70 mM) upon the suite of products formed from pyruvate in the presence of several transition metal sulfide minerals (Fig. 4B and Table S2). Alanine was formed in the presence of each mineral, although at strikingly different levels. This result does not accurately indicate the relative abilities of the minerals to facilitate this reaction, but rather their differential abilities to accelerate all of the competing reactions shown in Fig. 2. Nevertheless, it is clear that this reaction can be facilitated by a number of minerals, but that other reactions are more favorable under these conditions in each case. These results extend the findings of previous studies showing that FeS, $Fe(OH)_2$, and NiS are effective catalysts for reductive amination of α-keto acids at temperatures ranging from 20 to 100 °C (32, 33). ZnS also catalyzes reductive amination, but only in the presence of light (34), so this reaction is not relevant to chemistry at deep oceanic vents.

Summary

Transition metal sulfide minerals are capable of catalyzing the conversion of pyruvate to a number of products with moderate to high yields in only 24 h under relatively mild conditions. This finding supports the notion that hydrothermal vents were an important site for catalysis of chemical reactions. Conditions at extant hydrothermal vents vary considerably with respect to the types of minerals present, temperature, pH, and concentrations of reactive molecules such as H_2, H_2S, and NH_3. Although the conditions at primordial vents are not known, surely there was considerable variation at that time, as well. The results reported here begin to explore the effects of these variables on the reactivity landscape of pyruvate, an important biotic and presumably important prebiotic molecule. The results provide an illustration of the principle diagrammed in Fig. 1: the availability of catalysts and co-reactants both enables formation of reaction products and shapes the reaction network to favor certain suites of products. It is important for prebiotic chemists to address this inescapable complexity by defining the reactivity landscapes of various important molecules. Further, given the tendency for predominant formation of different products under different reaction conditions, it is important to capitalize upon what is known about the physical properties of hydrothermal vent systems to develop a picture of how molecules formed in one location might have been transported to other locations. Additional experiments that compare the intrinsic catalytic capabilities of different minerals and address the outcome of chemical reactions in the presence of mixed minerals are also needed to provide a more complete understanding of the factors that shape the topology of geochemical reaction networks at and surrounding hydrothermal vents.

Materials and Methods

Reactions of pyruvate were carried out by loading a one mL slurry containing powdered minerals, pyruvate and, in some cases, NH_4Cl, into the reactor shown in Figure 3 under anoxic conditions. Gases (H_2S, H_2, and CO_2) were introduced sequentially into the headspace above the Teflon tube. The vessel was pressurized and incubated with rocking at either room temperature of 110 °C for 24 hours. A detailed description of this procedure as well as procedures for recovery and analysis of reaction products are described in *SI Materials and Methods*.

1. Baross JA, Hoffman SE (1985) Submarine hydrothermal vents and associated gradient environments as sites for the origin and evolution of life. *Orig Life Evol Biosph* 15(4):327–345.
2. Budin I, Bruckner RJ, Szostak JW (2009) Formation of protocell-like vesicles in a thermal diffusion column. *J Am Chem Soc* 131(28):9628–9629.
3. Baaske P, et al. (2007) Extreme accumulation of nucleotides in simulated hydrothermal pore systems. *Proc Natl Acad Sci USA* 104(22):9346–9351.
4. Copley SD, Smith E, Morowitz HJ (2010) The emergence of sparse metabolic networks. *J Cosmol* 10:3345–3361.
5. Wächtershäuser G (1988) Before enzymes and templates: theory of surface metabolism. *Microbiol Rev* 52(4):452–484.
6. Martin W, Baross J, Kelley D, Russell MJ (2008) Hydrothermal vents and the origin of life. *Nat Rev Microbiol* 6(11):805–814.
7. Cody GD, et al. (2004) Assaying the catalytic potential of transition metal sulfides for abiotic carbon fixation. *Geochim Cosmochim Acta* 68:2185–2196.
8. Cody G (2004) Transition metal sulfides and the origin of metabolism. *Annu Rev Earth Planet Sci* 32:569–599.
9. Rees DC (2002) Great metalloclusters in enzymology. *Annu Rev Biochem* 71:221–246.
10. Satterfield CN (2008) *Heterogeneous catalysis in industrial practice.* (McGraw Hill, New York) 2nd Ed.
11. Kelley DS, Baross JA, Delaney JR (2002) Volcanoes, fluids, and life at mid-ocean ridge spreading centers. *Annu Rev Earth Planet Sci* 30:385–491.
12. Murnane R, Clague DA (1983) Nontronite from a low temperature hydrothermal system on the Juan de Fuca Ridge. *Earth Planet Sci Lett* 65(2):343–352.
13. Hrischeva E, Scott SD (2007) Geochemistry and morphology of metalliferous sediments and oxyhydroxides from the Endeavor segment, Juan de Fuca ridge. *Geochim Cosmochim Acta* 71(14):3476–3497.
14. Inoue A (2000) Two-dimensional variations of exchangeable cation composition in the terrigenous sediment, eastern flank of the Juan de Fuca Ridge. *Mar Geol* 162(2-4):501–528.
15. Floyd PA, ed (1986) *Petrology and Geochemistry of Oceanic Intraplate Sheet-Flow Basalts, Nauru Basin, Deep Sea Drilling Project Leg 89* (US Govt Printing Office, Washington, DC), 89, pp 471–497.
16. Kelley DS, et al. (2005) A serpentinite-hosted ecosystem: The Lost City hydrothermal field. *Science* 307(5714):1428–1434.
17. Kelley DS, et al.; AT3-60 Shipboard Party (2001) An off-axis hydrothermal vent field near the Mid-Atlantic Ridge at 30 degrees N. *Nature* 412(6843):145–149.
18. Cody GD, et al. (2000) Primordial carbonylated iron-sulfur compounds and the synthesis of pyruvate. *Science* 289(5483):1337–1340.
19. Brandes JA, et al. (1998) Abiotic nitrogen reduction on the early Earth. *Nature* 395(6700):365–367.
20. Kaschke M, Russell MJ, Cole WJ (1994) [FeS/FeS2], a redox system for the origin of life (some experiments on the pyrite-hypothesis). *Orig Life Evol Biosph* 24(1):43–56.
21. Connelly DP, et al. (2012) Hydrothermal vent fields and chemosynthetic biota on the world's deepest seafloor spreading centre. *Nat Commun* 3:620.
22. Rees DC, Howard JB (2003) The interface between the biological and inorganic worlds: Iron-sulfur metalloclusters. *Science* 300(5621):929–931.
23. Knowles WS, Noyori R (2007) Pioneering perspectives on asymmetric hydrogenation. *Acc Chem Res* 40(12):1238–1239.
24. McGregor WM, Sherrington DC (1993) Some recent synthetic routes to thioketones and thioaldehydes. *Chem Soc Rev* 22:199–204.
25. Chaffey-Miller H, Izgorodina EI, Barner-Kowollik C, Coote ML (2006) Radical addition to thioketones: Computer-aided design of spin traps for controlling free-radical polymerization. *J Chem Theory Comput* 2(6):1632–1645.
26. Soppa J (2010) Protein acetylation in archaea, bacteria, and eukaryotes. *Archaea* 2010:2010.
27. Polevoda B, Sherman F (2002) The diversity of acetylated proteins. *Genome Biol* 3(5): reviews0006.
28. Thao S, Escalante-Semerena JC (2011) Control of protein function by reversible Nε-lysine acetylation in bacteria. *Curr Opin Microbiol* 14(2):200–204.
29. Shisler KA, Broderick JB (2012) Emerging themes in radical SAM chemistry. *Curr Opin Struct Biol* 22(6):701–710.
30. Fontecave M, Atta M, Mulliez E (2004) S-adenosylmethionine: Nothing goes to waste. *Trends Biochem Sci* 29(5):243–249.
31. Blöchl E, Keller M, Wächtershäuser G, Stetter KO (1992) Reactions depending on iron sulfide and linking geochemistry with biochemistry. *Proc Natl Acad Sci USA* 89(17):8117–8120.
32. Hafenbradl D, Keller M, Wächtershäuser G, Stetter KO (1995) Primordial amino acids by reductive amination of a-oxo acids in conjunction with the oxidative formation of pyrite. *Tetrahedron Lett* 36:5179–5182.
33. Huber C, Wächtershäuser G (2003) Primordial reductive amination revisited. *Tetrahedron Lett* 44(8):1695–1697.
34. Wang W, Li Q, Liu X, Yang Y, Su W (2012) Enhanced photocatalytic performance of ZnS for reversible amination of α-oxo acids by hydrothermal treatment. *Orig Life Evol Biosph* 42(4):263–273.